

Published in final edited form as:

*Neurosci Lett.* 2007 July 11; 422(2): 136–140. doi:10.1016/j.neulet.2007.06.016.

## MOSSY CELL AXON SYNAPTIC CONTACTS ON ECTOPIC GRANULE CELLS THAT ARE BORN FOLLOWING PILOCARPINE-INDUCED SEIZURES

Joseph P. Pierce<sup>1</sup>, Michael Punsoni<sup>1</sup>, Daniel P. McCloskey<sup>2</sup>, and Helen E. Scharfman<sup>2,3</sup>

<sup>1</sup> Dept. of Neurology and Neuroscience, Weill Medical Coll. of Cornell Univ., New York, NY

<sup>2</sup> Center for Neural Recovery and Rehab. Res., Helen Hayes Hospital, West Haverstraw, NY

<sup>3</sup> Depts. of Pharmacology and Neurology, Columbia University, New York, NY

### Abstract

Granule cell neurogenesis increases following seizures, and some newly born granule cells develop at abnormal locations within the hilus. These ectopic granule cells (EGCs) demonstrate regular bursts of action potentials that are synchronized with CA3 pyramidal cell burst discharges and the bursts of hilar neurons, including mossy cells. Such findings suggest that mossy cells may participate in circuits that activate EGCs. Electron microscopic immunolabeling was therefore used to determine if mossy cell axon terminals form synapses with hilar EGC dendrites, using animals that underwent pilocarpine-induced status epilepticus. Pilocarpine was administered to adult male rats, and those which developed status epilepticus were perfused five to seven months later, after the period of EGC genesis. Hippocampal sections were processed for dual electron microscopic immunolabeling (using calcitonin gene-related peptide (CGRP) as a marker for mossy cells and calbindin (CaBP) as a marker for EGCs). Light microscopic analysis revealed large CGRP-immunoreactive cells in the hilus, with the appearance and distribution of mossy cells. Electron microscopic analysis revealed numerous CaBP-immunoreactive dendrites in the hilus, some of which were innervated by CGRP-immunoreactive terminals. The results suggest that mossy cells participate in the excitatory circuits which activate EGCs, providing further insight into the network rearrangements that accompany seizure-induced neurogenesis in this animal model of epilepsy.

### Keywords

Dentate Gyrus; Neurogenesis; CGRP; Pilocarpine; Status Epilepticus; Temporal Lobe Epilepsy

---

Granule cell (GC) neurogenesis in the dentate gyrus increases following seizures (for a review see [19, 29]), with a substantial number of newly-generated GCs [13] migrating abnormally into the hilus after status epilepticus [7, 18, 20, 27, 31]. Anatomical and physiological studies indicate that these ectopic GCs (EGCs) are able to insert themselves into hilar circuitry [7, 15, 27, 35, 36]. For example, EGCs are innervated by mossy fibers (the axons of GCs) [7], a projection which represents a prime source of afferent input to

---

Corresponding Author: Joseph P. Pierce, Dept. of Neurology and Neuroscience, Weill Medical Coll. of Cornell Univ., 411 E 69th St., New York, NY 10021, Phone: (212) 5700 #339, Fax: (212) 988-3672, jppierc@med.cornell.edu.

**Publisher's Disclaimer:** This is a PDF file of an unedited manuscript that has been accepted for publication. As a service to our customers we are providing this early version of the manuscript. The manuscript will undergo copyediting, typesetting, and review of the resulting proof before it is published in its final form. Please note that during the production process errors may be discovered which could affect the content, and all legal disclaimers that apply to the journal pertain.

EGCs [22]. In addition, EGCs are activated by perforant path stimulation [35], and following a spontaneous limbic seizure *in vivo*, *c-fos* is expressed in EGCs [36]. The fact that EGCs are a functional component of hippocampal circuitry is further exemplified by the observation that synchronized bursts of action potentials occur in EGCs, area CA3 neurons, and other hilar cells [31, 34].

However, the ways that hilar cells interact with EGCs are still not clear. One could predict that hilar mossy cells would be likely to innervate hilar EGCs, since mossy cells have hilar axon collaterals, and normally project to GCs [5, 12, 26]. Although mossy cells are particularly vulnerable following seizures [32, 33, 37], and their loss has been implicated in epileptogenesis [37], many can survive [34]. To determine if the hilar collaterals of surviving mossy cells could sprout onto developing EGC dendrites, prebedding dual electron microscopic (EM) immunolabeling was used, employing calcitonin gene-related peptide immunoreactivity (CGRP-IR) as a selective marker for mossy cells and their axon terminals [6, 8], and calbindin D<sub>28K</sub> (CaBP)-IR as a selective marker for EGC dendrites [22, 24, 30, 31] in the hilus. CaBP does label some interneurons in the hippocampus, but such neurons are rare in the dentate gyrus [10, 31, 34]. Additionally, following pilocarpine-induced status epilepticus, double labeling of hilar tissue for CaBP and Prox-1 (a granule cell specific marker) revealed no CaBP labeled cells that were not also labeled for Prox-1 [30].

The pilocarpine model of epilepsy was used to generate status epilepticus and recurrent seizures. Status epilepticus was truncated at 1 hr by anticonvulsant administration, since this generates animals with a robust population of hilar EGCs [13, 31], survival of many mossy cells [34], and recurrent seizures with pronounced synaptic reorganization [31, 36]. Specifically, adult male Sprague Dawley rats (180–240 g, approximately 42 days old) were injected with atropine methylbromide (1 mg/kg s.c.) and 30 min later with pilocarpine hydrochloride (380 mg/kg i.p.). The onset of status epilepticus was defined as the first series of stage 5 seizures [23] that did not abate after 5 min. Diazepam (5 mg/kg i.p., Wyeth-Ayerst) was injected 1 hr after the onset of status epilepticus. After 5 hr, animals were injected with 2.5 ml 5% dextrose in lactate-ringer's s.c. (see [36] for other details of the methods). All animals used in this study had recurrent spontaneous behavioral seizures. Saline controls (the same age as the pilocarpine-treated rats) received identical treatment (atropine and diazepam), but were injected with saline instead of convulsant. Animal care and use followed the guidelines set by the N.I.H. Guide for the Care and Use of Laboratory Animals. All efforts were made to minimize both the number of animals, and any discomfort to the animal. Five to seven months after seizure induction, a time when animals have developed recurrent spontaneous seizures and EGC numbers are stable [13], animals were injected with an overdose of pentobarbital (150 mg/kg i.p.) and sequentially perfused with a saline-heparin solution, 3.75% acrolein and 2% paraformaldehyde (PF) in 0.1 M phosphate buffer (PB) and 2% PF in PB. Brains were then blocked and postfixed in 2% PF in PB. Vibratome sections (40  $\mu$ m) through the hippocampal formation were cut into cold PB, transferred to a storage solution (30% sucrose and 10% ethylene glycol in 0.1 M PB) and stored at  $-25^{\circ}$  C. Random systematic series of sections (1 in 10) from each animal were then processed in parallel to concurrently label CGRP with immunoperoxidase (ImP) and CaBP with immunogold (ImG). Following sodium borohydride and freeze-thaw treatments (for procedural details see [22]), and incubation in a 0.5% bovine serum albumin (BSA) solution, tissue was placed in an antibody cocktail containing: 1) a rabbit anti-rat CGRP antibody (Peninsula Labs Inc., #IHC6006, 1:5000; whose specificity has been demonstrated on tissue from CGRP-null mice [17]), and 2) a mouse monoclonal CaBP D<sub>28K</sub> antibody (Sigma-Aldrich Inc., clone CB-955, 1:200; whose specificity has also been extensively tested, and which can clearly label EGCs and their processes in the hilus [22, 31]) for 48 hrs. Processes containing CGRP were then ImP-labeled with the avidin-biotin-peroxidase

complex method [11], using the following incubations separated by rinses: (a) a 1:400 dilution of goat anti-rabbit biotinylated-IgG in 0.1% BSA/tris saline (TS), 30 min (Jackson Immunoresearch, West Grove, PA), (b) a 1:100 dilution of avidin-biotin-peroxidase complex in 0.05% BSA/TS (Vectastain Elite Kit, Vector Laboratories, Burlingame, CA), 30 min, (c) 0.022% 3,3'-diaminobenzidine and 0.003% H<sub>2</sub>O<sub>2</sub> in TS, 8 min, and (d) a PB wash, 10 min. Sections were further processed to ImG-label CaBP through: (a) PB saline (PBS, 0.9% NaCl in 0.01 M PB, pH 7.4), 10 min, (b) blocking buffer (0.8% BSA and 0.1% gelatin in PBS), 10 min, (c) 1 nm gold particle-conjugated goat anti-mouse IgG (Amersham, Arlington Heights, IL) in blocking buffer, 18 hr; (d) blocking buffer, 5 min, (e) PBS rinses and postfixation in 2% glutaraldehyde, 10 min, (f) citrate buffer (0.2 M, pH 7.4), 10 min, (g) silver intensification using an IntenSE-M Kit (Amersham, Arlington Heights, IL), 7 min, and (i) citrate buffer wash, 10 min. Preparation for EM examination involved: (a) PB wash, 5 min, (b) postfixation in 2% osmium, 1 hr, (c) dehydration in a series of graded alcohols and propylene oxide, (d) 1:1 Embed 812 (Electron Microscopy Sciences Inc., Hatfield, PA) and propylene oxide, 12 hr, (e) 100% Embed 812, 2 hrs, (f) flat-embedding between Aclar film (Allied Signal, Pottsville, PA), and (g) polymerization at 60° C, 72 hr. Non-selective ImG labeling levels were estimated by normal processing with omission of that primary antibody.

Select portions of the hilar subfield of the dentate gyrus were excised after embedding. These were trimmed, resectioned (65 nm), collected on copper grids, and counterstained with uranyl acetate and lead citrate [25] prior to examination on a Technai transmission electron microscope (FEI Company, Hillsboro, OR). Sections containing CGRP ImP-labeled cells were selected for analysis since the density of mossy cell hilar axonal arbors would presumably be greatest in these sections, providing an increased likelihood of finding contacts with EGC dendrites. Four sections per animal, on different grids, were analyzed for 3 different experimental animals and 2 saline controls. Profiles were categorized based on the criteria of Peters et al. [21]. To obtain optimal labeling and control for the effect of penetration, only ultrastructural fields which were adjacent to the plastic/tissue interface were examined [2]. All dendritic profiles containing two or more gold particles (CaBP labeling) in portions of grid squares that displayed no tissue damage were analyzed, to determine if they formed synapses with axon terminals containing ImP labeling (for CGRP). Digital images were captured with an AMT Advantage HR/HR-B CCD Camera System (Advanced Microscopy Techniques, Danvers, MA), and printed using a Tektronix phaser 860 printer. All figures were assembled in Photoshop 7.0 (Adobe Inc., San Jose, CA).

Light microscopic analysis of the hilus of embedded tissue from pilocarpine-treated animals revealed the presence of large CGRP-IR neurons (Fig. 1) that were comparable in both appearance and distribution to mossy cells in normal adult rats, as previously described [1, 26], particularly when visualized with CGRP immunolabeling [6, 8]. The somata of CGRP-IR cells displayed average diameters of  $22 \pm 3 \mu\text{m}$  (major axis,  $n = 21$ ) and  $16 \pm 3$  (minor axis), slightly larger than the values reported by Freund et al. [8] for normal animals, possibly because larger mossy cells might be more likely to survive status epilepticus. Faintly-labeled dendrites of mossy cells extended from the somata in triangular or bipolar patterns in the plane of section, similar to previously-described mossy cells [1, 26]. Mossy cells were observed in subgranular and central portions of the hilus at both dorsal and ventral levels, but were more frequent ventrally, in accord with previous reports [4, 8]. Labeling was detected in the inner molecular layer (ML), but it was faint, probably because it was partially obscured by osmication. CGRP-IR neurons in saline control tissue had a similar appearance and distribution.

Using standard light microscopic techniques, CaBP-ImG labeling was barely detectable. However, oblique illumination, which reflects light from ImG particles, revealed numerous

CaBP-labeled somata and dendrites in both the dorsal and ventral hilus of pilocarpine-treated animals, whose distribution matched previous reports that used CaBP-ImP labeling [22, 31]. Such labeling was not observed in the hilus of control animals. At the ultrastructural level, ImG-labeled EGC dendritic profiles were common in the hilus of pilocarpine-treated animals, and not evident in the hilus of control animals. Their pattern of distribution resembled previous observations made with the same immunolabeling protocol [22]. The overall density of labeling in the neuropil was  $0.172 \pm 0.018$  ImG particles per  $\mu\text{m}^2$  (measured in 4 grid squares,  $12,104 \mu\text{m}^2$ , from two animals), compared to a density of  $0.008 \pm 0.001$  ImG particles per  $\mu\text{m}^2$  (measured in a comparable area) when the same labeling protocol was applied, with the primary antibody omitted. This suggests that only 5% of ImG particles reflect non-specific labeling. The surfaces of ImG-labeled dendritic profiles were primarily covered with axon terminals, many of which formed synapses with the dendrite in the plane of section (Fig. 2). Some terminals also contained ImG particles, identifying them as mossy fiber terminals (as granule cell axons, mossy fibers contain CaBP). CGRP ImP-labeled axon terminals also contacted ImG-labeled EGC dendrites (Fig. 2). Across a total of  $245,094 \mu\text{m}^2$  (81 grid squares) of neuropil examined, 18 such contacts were observed, 6 of which displayed synapses in the plane of section. These terminals tended to be small and contacted the dendritic shaft, as previously observed for mossy cell terminals in the hilus [5, 26, 38]. CGRP ImP-labeling was often concentrated over dense core vesicles (DCVs), when they were visible in the plane of section (Fig. 2b), but diffuse ImP labeling within the terminal could at times also be observed, presumably as a result of CGRP leakage from DCVs during tissue processing. This pattern of labeling is virtually identical to previous reports of CGRP-labeled mossy cell axon terminals [6, 8]. When a synapse was observed between the terminal and dendrite, the postsynaptic density appeared to be less pronounced than a classic type 1 asymmetric synapse [9], although a distinct postsynaptic density was always present (in contrast to type 2 symmetric synapses, where the density is often absent, and which are best identified by the presence of filamentous material in the synaptic cleft and apposed presynaptic vesicles [21]). Mossy fiber terminals which contact EGC dendrites also often have thin postsynaptic densities [22], suggesting that this might be a characteristic feature of excitatory contacts on EGC dendrites.

These findings demonstrate that hilar mossy cells innervate EGC dendrites in the hilus of pilocarpine-treated animals with recurrent seizures. The density of innervation is difficult to predict since CGRP-ImP labeling could be restricted within terminals, making them difficult to detect and presumably resulting in an underestimation of the number of labeled terminals. However, the fact that these connections exist indicates new ways that EGCs can integrate with preexisting neurons in the dentate gyrus. Thus, they are not only innervated by GCs, but also surviving mossy cells. Innervation by mossy cells may be stimulated by the fact that some adjacent interneurons die after status epilepticus [3, 16], and many EGCs develop in the areas where the interneurons were located. The axons of surviving hilar mossy cells may respond to the loss of their normal hilar targets by contacting nearby EGCs. These novel synaptic interactions will require more analysis before their functional effect is completely clear. Indeed, if a thin specialization characterizes this type of synapse the functional effect may be atypical. However, if the connections observed in this study are active glutamatergic synapses, the pathway from mossy cell to EGC could have important implications. First, it would be likely to increase network excitability, since it represents enhanced excitatory connectivity. Second, it may explain why CA3 pyramidal cells exhibit burst discharges that are synchronized with both EGCs [31] and surviving mossy cells [34]. Mossy cells receive some input from CA3 pyramidal cell axon collaterals [14, 28], which could then activate EGCs. In addition, it could help elucidate why perforant path stimulation evokes robust excitatory postsynaptic potentials in hilar EGCs even when EGCs lack dendrites in the ML [35]. Perforant path fibers that innervate granule cells and mossy cells with ML dendrites could excite hilar EGCs disynaptically or polysynaptically [35].

The data presented here thus supports the hypothesis that increased recurrent excitatory circuitry develops in the pilocarpine animal model of epilepsy [15, 35], which could contribute to seizures in these animals. However, regardless of the implications for epilepsy, these results increase our understanding of the ways seizure-induced neurogenesis affects the dentate gyrus: it generates ectopic neurons which integrate into the dentate gyrus network in diverse and robust ways, i.e., through synaptic connections formed with many different cell types in the region, not just other granule cells.

## Acknowledgments

This research was supported by NIH NS 41490, the Epilepsy Foundation, and the Helen Hayes Hospital Foundation.

## References

1. Amaral DG. A Golgi study of the cell types in the hilar region of the hippocampus in the rat. *J Comp Neurol.* 1978; 182:851–914. [PubMed: 730852]
2. Auchus AP, Pickel VM. Quantitative light microscopic demonstration of increased pallidal and striatal Met<sup>5</sup>-enkephalin like immunoreactivity in rats following chronic haloperidol but not with clozapine. *Exp Neurol.* 1992; 117:17–27. [PubMed: 1618284]
3. Ben-Ari Y. Limbic seizure and brain damage produced by kainic acid: mechanisms and relevance to human temporal lobe epilepsy. *Neuroscience.* 1985; 14:375–403. [PubMed: 2859548]
4. Buckmaster PS, Jongen-Reilo AL. Highly specific neuron loss preserves lateral inhibitory circuits in the dentate gyrus of kainate-induced epileptic rats. *J Neurosci.* 1999; 19:9519–9529. [PubMed: 10531454]
5. Buckmaster PS, Wenzel HJ, Kunkel DD, Schwartzkroin PA. Axonal arbors and synaptic connections of hippocampal mossy cells in the rat in vivo. *J Comp Neurol.* 1996; 366:271–292. [PubMed: 8698887]
6. Bulloch K, Prasad A, Conrad CD, McEwen BS, Milner TA. Calcitonin gene-related peptide level in the rat dentate gyrus increases after damage. *NeuroReport.* 1996; 7:1036–1040. [PubMed: 8804046]
7. Dashtipour K, Tran PH, Okazaki MM, Nadler JV, Ribak CE. Ultrastructural features and synaptic connections of hilar ectopic granule cells in the rat dentate gyrus are different from those of granule cells in the granule cell layer. *Brain Res.* 2001; 890:261–271. [PubMed: 11164792]
8. Freund TF, Hajos N, Acsady L, Gorcs TJ, Katona I. Mossy cells of the rat dentate gyrus are immunoreactive for calcitonin gene-related peptide (CGRP). *Eur J Neurosci.* 1997; 9:1815–1830. [PubMed: 9383204]
9. Gray EG. Axo-somatic and axo-dendritic synapses of the cerebral cortex: an electron microscope study. *J Anat.* 1959; 93:420–433. [PubMed: 13829103]
10. Gulyas AI, Toth K, Danos P, Freund TF. Subpopulations of GABAergic neurons containing parvalbumin, calbindin D28k, and cholecystokinin in the rat hippocampus. *J Comp Neurol.* 1991; 312:371–378. [PubMed: 1721075]
11. Hsu SM, Raine L, Fanger H. Use of avidin-biotin-peroxidase complex (ABC) in immunoperoxidase techniques: a comparison between ABC and unlabeled antibody (PAP) procedures. *J Histochem Cytochem.* 1981; 29:557–580.
12. Laurberg S, Zimmer J. Lesion-induced sprouting of hippocampal mossy fiber collaterals to the fascia dentata in developing and adult rats. *J Comp Neurol.* 1981; 200:433. [PubMed: 7276246]
13. McCloskey D, Hintz TM, Pierce JP, Scharfman HE. Stereological methods reveal the robust size and stability of ectopic hilar granule cells after pilocarpine-induced status epilepticus in the adult rat. *Euro J of Neurosci.* 2006; 24:2203–2210.
14. Muller W, Misgeld U. Picrotoxin- and 4-aminopyridine-induced activity in hilar neurons in the guinea pig hippocampal slice. *J Neurophysiol.* 1991; 65:141–147. [PubMed: 1999728]
15. Nadler JV. The recurrent mossy fiber pathway of the epileptic brain. *Neurochem Res.* 2003; 28:1649–1658. [PubMed: 14584819]

16. Nadler JV, Evenson DA, Cuthbertson GJ. Comparative toxicity of kainic acid and other acidic amino acids toward rat hippocampal neurons. *Neurosci.* 1981; 6:2505–2519.
17. Oh-hashii Y, Shindo T, Kurihara Y, Imai T, Wang Y, Morita H, Imai Y, Kayaba Y, Nishimatsu H, Suematsu Y, Hirata Y, Yazaki Y, Nagai R, Kuwaki T, Kurihara H. Elevated sympathetic nervous activity in mice deficient in alphaCGRP. *Circ Res.* 2001; 89:983–990. [PubMed: 11717154]
18. Parent JM, Elliott RC, Pleasure SJ, Barbaro NM, Lowenstein DH. Aberrant seizure-induced neurogenesis in experimental temporal lobe epilepsy. *Ann Neurol.* 2006; 59:81–91. [PubMed: 16261566]
19. Parent JM, Lowenstein DH. Seizure-induced neurogenesis: are more new neurons good for an adult brain? *Prog Brain Res.* 2002; 135:121–131. [PubMed: 12143334]
20. Parent JM, Yu TW, Leibowitz RT, Geshwind DH, Sloviter RS, Lowenstein DH. Dentate granule cell neurogenesis is increased by seizures and contributes to aberrant network reorganization in the rat. *J Neurosci.* 1997; 17:3727–3728. [PubMed: 9133393]
21. Peters, A.; Palay, S.L.; Webster, H. *The Fine Structure of the Nervous System: the Neurons and Supporting Cells.* W.B. Saunders Co; Philadelphia: 1991. p. 157
22. Pierce JP, Melton J, Punsoni M, McCloskey DP, Scharfman HE. Mossy fibers are the primary source of afferent input to ectopic granule cells that are born after pilocarpine-induced seizures. *Exp Neurol.* 2005; 196:316–331. [PubMed: 16342370]
23. Racine RC. Modification of seizure activity by electrical stimulation: II. Motor seizure. *Electroenceph clin Neurophysiol.* 1972; 32:281–294. [PubMed: 4110397]
24. Rami A, Brehier A, Thomasset M, Rabie A. The comparative immunocytochemical distribution of 28 kDa cholecalciferin (CaBP) in the hippocampus of rat, guinea pig and hedgehog. *Brain Res.* 1987; 422:149–153. [PubMed: 3676777]
25. Reynolds ES. The use of lead citrate at high pH as an electron-opaque stain in electron microscopy. *J Cell Bio.* 1963; 17:208–212. [PubMed: 13986422]
26. Ribak CE, Seress L, Amaral DG. The development, ultrastructure and synaptic connections of the mossy cells of the dentate gyrus. *J Neurocytol.* 1985; 14:835–857. [PubMed: 2419523]
27. Ribak CE, Tran PH, Spigelman I, Okazaki MM, Nadler JV. Status epilepticus-induced hilar basal dendrites on rodent granule cells contribute to recurrent excitatory circuitry. *J Comp Neurol.* 2000; 428:240–253. [PubMed: 11064364]
28. Scharfman HE. EPSPs of dentate gyrus granule cells during epileptiform bursts of dentate hilar “mossy” cells and area CA3 pyramidal cells in disinhibited rat hippocampal slices. *J Neurosci.* 1994; 14:6041–6057. [PubMed: 7931561]
29. Scharfman HE. Functional implications of seizure-induced neurogenesis. *Adv Exp Med Biol.* 2004; 548:192–212. [PubMed: 15250595]
30. Scharfman HE, Goodman JH, McCloskey DP. Ectopic granule cells of the rat dentate gyrus. *Dev Neurosci.* 2007; 29:14–27. [PubMed: 17148946]
31. Scharfman HE, Goodman JH, Sollas AL. Granule-like neurons at the hilar/CA3 border after status epilepticus and their synchrony with area CA3 pyramidal cells: functional implications of seizure-induced neurogenesis. *J Neurosci.* 2000; 20:6144–6158. [PubMed: 10934264]
32. Scharfman HE, Schwartzkroin PA. Protection of dentate hilar cells from prolonged stimulation by intracellular calcium chelation. *Science.* 1989:257–260. [PubMed: 2508225]
33. Scharfman HE, Schwartzkroin PA. Responses of cells of the rat fascia dentata to prolonged stimulation of the perforant path: Sensitivity of hilar cells and changes in granule cell excitability. *Neuroscience.* 1990; 35:491–504. [PubMed: 2381513]
34. Scharfman HE, Smith KL, Goodman JH, Sollas AL. Survival of dentate hilar mossy cells after pilocarpine-induced seizures and their synchronized burst discharges with area CA3 pyramidal cells. *Neuroscience.* 2001; 104:741–759. [PubMed: 11440806]
35. Scharfman HE, Sollas AE, Berger RE, Goodman JH, Pierce JP. Perforant path activation of ectopic granule cells that are born after pilocarpine-induced seizures. *Neuroscience.* 2003; 121:1017–1029. [PubMed: 14580952]
36. Scharfman HE, Sollas AL, Goodman JH. Spontaneous recurrent seizures after pilocarpine-induced status epilepticus activate calbindin-immunoreactive hilar cells of the rat dentate gyrus. *Neuroscience.* 2002; 111:71–81. [PubMed: 11955713]

37. Sloviter RS. Permanently altered hippocampal structure, excitability, and inhibition after experimental status epilepticus in the rat: The “dormant basket cell” hypothesis and its possible relevance to temporal lobe epilepsy. *Hippocampus*. 1991; 1:41–66. [PubMed: 1688284]
38. Wenzel HJ, Buckmaster PS, Anderson NL, Wenzel ME, Schwartzkroin PA. Ultrastructural localization of neurotransmitter immunoreactivity in mossy cell axons and their synaptic targets in the rat dentate gyrus. *Hippocampus*. 1997; 7:559–570. [PubMed: 9347352]

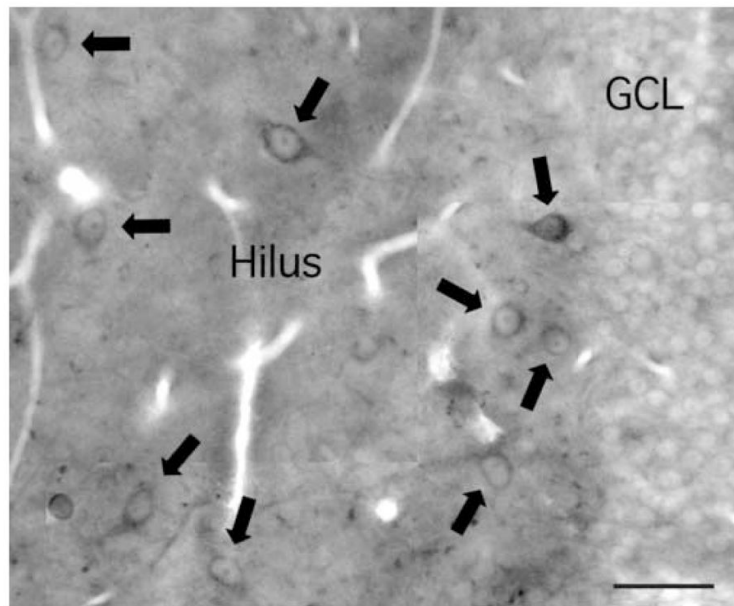


**Fig. 1.** Numerous large CGRP-IR neurons are visible in this composite light microscopic image of the ventral dentate gyrus of a pilocarpine-treated animal. GCL, Granule Cell Layer, Scale Bar = 50  $\mu$ m.

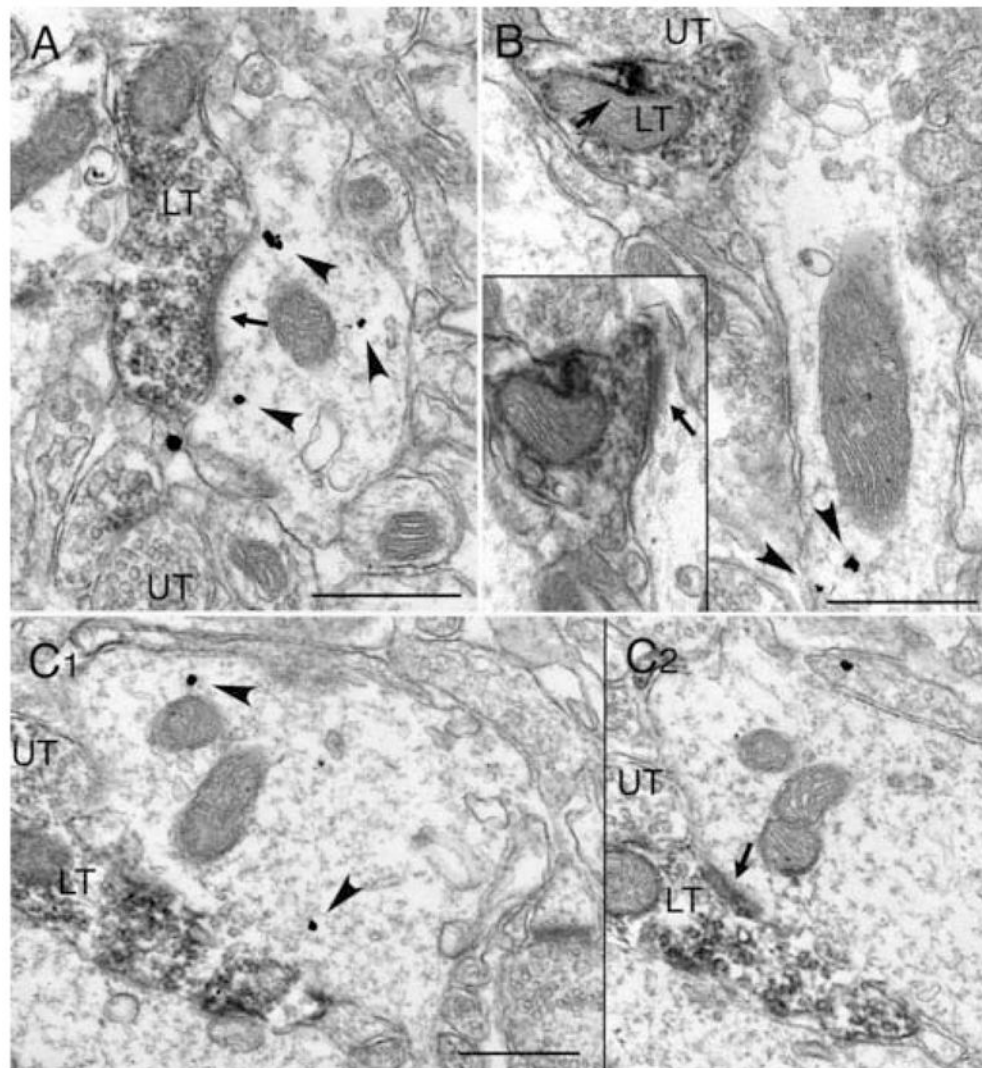


**Fig. 2.** Hilar CGRP ImP-labeled terminals (LT) form synaptic contacts (small arrows) with EGC dendrites, defined by CaBP-ImG labeling (arrowheads). Unlabeled terminals (UT) are noted for comparison. A CGRP ImP-labeled DCV is present in panel B (large arrow). CaBP-ImG labeling is also present in axonal processes (unmarked ImG particles in A and C), reflecting axons of CaBP-labeled granule cells and EGCs in the hilus. The inset in B shows the labeled terminal tilted to 50° to better display the synapse. In C1, a CGRP ImP-labeled terminal is apposed to a CaBP-ImG labeled dendrite. In C2, two sections from C1, these processes form a synaptic contact. Scale Bar = 500 nm.